

1 Observed Kinetics of Enterovirus Inactivation by Free Chlorine 2 Is Host Cell-Dependent

3

4 Shotaro Torii*, Shannon Christa David, Odile Larivé, Federica Cariti, Tamar Kohn

5

6 Laboratory of Environmental Chemistry, School of Architecture, Civil and
7 Environmental Engineering (ENAC), École Polytechnique Fédérale de Lausanne
8 (EPFL), Lausanne, Switzerland

9

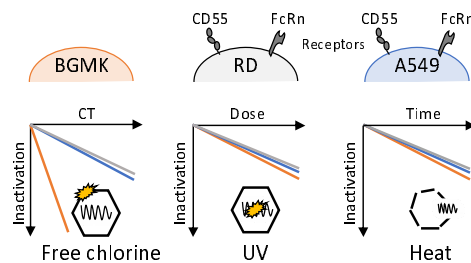
10 *Corresponding author: Shotaro Torii

11 Email address: shotaro.torii@epfl.ch

12

13

14 Graphic for Table of Contents (TOC)



15

16

17 **Abstract**

18 The virucidal efficacy of disinfectants is typically assessed by infectivity assay
19 utilizing a single type of host cell. Enteroviruses infect multiple host cells via different
20 entry routes, and each entry route may be impaired to a varying extent by a given
21 disinfectant. Yet, it is not known how the choice of host cells for titration affects the
22 observed inactivation kinetics. Here, we evaluated the inactivation kinetics of echovirus
23 11 (E11) by free chlorine, ultraviolet (UV) irradiation, and heat, using three different
24 host cells (BGMK, RD, and A549). E11 inactivation by free chlorine occurred at a
25 two-fold greater rate when enumerated on BGMK cells compared to RD and A549 cells.
26 Conversely, a comparable inactivation rate was observed for UV and heat independent
27 of the host cell used. Host cell-dependent inactivation kinetics by free chlorine were
28 also observed for echovirus 7, 9 and 13, and coxsackievirus A9, confirming that this
29 phenomenon is not serotype-specific. Inactivation of E11 was partly caused by a loss in
30 host cell attachment, which was most pronounced for BGMK cells, and which may be
31 promoted by a lack of CD55 attachment receptors on this cell type. Additionally,
32 BGMK cells lack a key subunit of the uncoating receptor, β 2M, which may further
33 contribute to the differential inactivation kinetic for this cell type. Consequently,
34 inactivation kinetics of enteroviruses should be assessed using host cells with different
35 receptor profiles. This will yield a more complete understanding of the inactivating
36 power of disinfectants targeting the viral attachment and/or uncoating.

37 **Keywords**

38 Virus; Disinfection; Free chlorine; Host Cells; Inactivation; Water treatment

39 Introduction

40 Enteroviruses are non-enveloped positive single-stranded (ss) RNA viruses
41 comprising more than 100 serotypes that infect humans and can cause serious diseases ¹.
42 These viruses are excreted from the feces of infected persons into the sewage system,
43 and are often detected in wastewater and surface waters ², and have even been reported
44 in tap water after disinfection ³. Enteroviruses are therefore included as microbial
45 contaminants in the Draft Contaminant Candidate List 5 published by the US
46 Environmental Protection Agency (USEPA). Due to their ubiquity, enterovirus
47 inactivation during water and wastewater disinfection has been extensively studied ⁴⁻¹⁰.

48 To evaluate the virucidal efficacy of various disinfectants, methods relying on the
49 infection of a host cell are utilized (e.g., plaque assay and endpoint dilution assay).
50 Buffalo green monkey kidney (BGMK) cells ¹¹ are most commonly used for enterovirus
51 titration to assess the efficacy of disinfection in water treatment ^{4,7,8,12-17}. This is
52 assumingly because BGMK cells are the most efficient for enterovirus isolation ¹⁸ and
53 are employed to perform EPA method 1615 ^{19,20} which quantifies “total culturable virus”
54 in water samples. The use of BGMK cells is a *de facto* standard for the measurement of
55 infectious enterovirus in disinfection studies.

56 However, many enteroviruses are known to infect not only one but multiple types of
57 host cells. For example, one serotype of *Enterovirus*, echovirus type 11 (E11) is also
58 able to infect human rhabdomyosarcoma (RD) ²¹ and human alveolar basal epithelial
59 (A549) cells ^{22,23}. The infection starts by virus attachment to host cells. Previous studies
60 have found that the decay-accelerating factor (DAF or CD55) is an attachment receptor
61 for several enteroviruses, including E11 ²⁴. While viral attachment to CD55 enhances
62 the efficiency of infection, cells are still permissive to E11 infection even after the
63 suppression of CD55 by gene knockout or by blocking antibodies ^{25,26}. Importantly, E11
64 readily infects BGMK cells which lack CD55 on their surface ²⁷, indicating that E11 can
65 attach to host cells via multiple receptors. To trigger entry into the host, the virus must
66 additionally interact with an uncoating receptor, such as neonatal Fc receptor (FcRn)
67 ^{26,28}, which is a major histocompatibility complex class I-like protein comprising a
68 heavy α chain and a light β 2-microglobulin (β 2M) ^{29,30}. β 2M is also reported to be
69 essential for E11 infection on specific types of host cells (e.g., HEK293T, human

70 osteosarcoma U2OS cell line, and RD cells)^{25,26,28}; however, no studies have
71 investigated the expression of FcRn and its impact on E11 infectivity on BGMK cells.

72 Disinfectants inactivate viruses by inhibiting one or more viral functionalities,
73 including attachment to cells, entry into cells (i.e., uncoating), and genome replication.
74 The principle mechanism of inactivation differs depending on the disinfectant of interest
75 ³¹; free chlorine and heat mainly impair the attachment function of E11 while ultraviolet
76 irradiation (UV) mainly damages viral RNA, driving the loss of the replicative function
77 ^{32,33}. As host cell receptors can be highly variable across cell types, we expect
78 inactivation kinetics to differ depending on the host cells when assessing disinfectants
79 that target the viral attachment or uncoating stage. However, the effect of host cell
80 choice has only been studied for a disinfectant targeting the replicative function (UV
81 irradiation) using adenovirus ³⁴.

82 Here, we assessed the inactivation kinetics of a model enterovirus (E11 Gregory
83 strain) by free chlorine, UV irradiation, and heat, by individual enumeration using three
84 different types of host cells (BGMK, RD, and A549 cells) that are all permissive to
85 enterovirus infection. We also characterized the receptor profiles of these cells to
86 investigate the mechanism of the host cell-dependent inactivation kinetics. Finally, we
87 tested additional serotypes (echovirus 7, 9, 13 (E7, E9, and E13), coxsackievirus A9, B1
88 (CVA9 and CVB1)) to generalize our findings to other members of the *Enterovirus*
89 genus.

90 **Materials and Methods**

91 **Cells and Viruses**

92 BGMK and A549 cells were kindly provided by Spiez Laboratory and the Lausanne
93 University Hospital, Switzerland, respectively. RD cells were purchased from the
94 American Type Culture Collection (ATCC) (CCL-136). BGMK cells were grown in
95 Minimum Essential Medium (MEM; Gibco, UK) while A549 and RD cells were grown
96 in Dulbecco's Modified Eagle Medium (DMEM; Gibco). Both media types were
97 supplemented with 10% fetal bovine serum (FBS; Gibco) and 1%
98 penicillin-streptomycin (P/S; Gibco), and cells were incubated at 37°C with 5% CO₂.

99 E11 Gregory strain (ATCC VR-41) and CVB1 environmental isolate (Accession No.:
100 MG845887)¹⁵ were propagated on BGMK cells maintained in MEM supplemented
101 with 2% FBS and 1% P/S. E7, E9, E13, and CVA9 were kindly provided by Soile
102 Blomqvist and Carita Savolainen-Kopra (Finnish National Institute for Health and
103 Welfare) and were propagated on RD cells maintained in DMEM supplemented with
104 2% FBS and 1% P/S. All viruses were allowed to propagate in cells for 3 days, after
105 which the cell flasks were frozen at -80°C and then thawed at room-temperature. The
106 infected cell suspension was centrifuged at 3,000 × g for 15 min. The supernatant was
107 filtered through a 0.45 µm low protein binding durapore membrane (Merck Millipore
108 Ltd., Ireland). 20 mL of the filtrate was then ultracentrifuged at 150,000 × g at 4°C for 3
109 h (Beckman Coulter, USA) through a 20% (w/v) sucrose cushion. The pellets were
110 resuspended with a 500 µL of phosphate buffer (PB; 1 mM, pH 7.0) (United Chemical
111 Technologies, USA). The suspension was further filtered with a 0.22 µm hydrophilic
112 PTFE membrane (BGB Analytik AG, Switzerland). A 500 µL of PB was further filtered
113 to collect the remained virus on the membrane. The purified stock was stored at 4°C
114 before disinfection experiments. The concentrations of purified stocks were enumerated
115 as detailed below and reported in Table S1 in Supporting Information (SI).

116 **Enumeration of Infectious Viruses**

117 The concentrations of infectious viruses were quantified by endpoint dilution assay

118 using BGMK, RD, and A549 cells in 96-well plates as previously described³⁵. In brief,
119 the samples were serially diluted 10-fold in the corresponding maintenance medium
120 (MEM or DMEM, both of which were supplemented with 2% FBS and 1% P/S) Then,
121 150 μ L of the diluted samples were inoculated on the host cells, with five replicates per
122 dilution. After incubation at 37°C with 5% CO₂ for five days, the presence of a
123 cytopathic effect (CPE) in each well was checked by microscopy. The number of
124 positive wells showing CPE for each dilution was counted and converted to adjusted
125 most probable numbers (MPN) using the R package {MPN}³⁶. The lower limit of
126 detection (LoD) was defined as the concentration where CPE was observed at one out of
127 five wells at the lowest dilution, corresponding to 12 MPN/mL in this study.

128 Disinfection Experiments

129 Disinfection experiments were run in duplicate or triplicate for each virus-disinfectant
130 pair tested here. For each run, a total of three time-series samples plus an untreated
131 sample (i.e. sample at time zero), were taken. All experiments were conducted in
132 disinfectant demand-free 1 mM PB (pH 7.0). After the experiment, untreated and
133 disinfected samples were stored at 4°C for a maximum of 24h, then each sample was
134 split into three individual aliquots and was enumerated on each of the three host cell
135 types.

136

137 *Free Chlorine*

138 The free chlorine disinfection experiment was conducted in a batch system. A free
139 chlorine working solution was prepared by diluting sodium hypochlorite (Reactolab SA,
140 Switzerland) in 1 mM PB (pH 7.0). The final free chlorine concentration in the working
141 solution ranged from 0.54 to 0.57 mg L⁻¹. The free chlorine concentration was
142 measured by the *N, N*-diethyl-*p*-phenylenediamine (DPD) method³⁷ using a DR300
143 Chlorine Pocket Colorimeter (Hach Company, USA). Before each run, glass beakers
144 were soaked with >50 mg L⁻¹ of sodium hypochlorite overnight to quench the residual
145 chlorine demand. The beakers were rinsed twice with MilliQ water and once with the
146 chlorine working solution. Then, 10 - 50 μ L of virus stock solution was spiked into 11.5
147 mL of the working solution under constant stirring in the quenched beakers. A 500 μ L

148 aliquot was collected every 10–50 s (depending on the virus) and mixed with 5 μL of
149 5,000 mg L^{-1} sodium thiosulfate (Sigma-Aldrich, Germany) to instantly quench the
150 residual free chlorine. The free chlorine concentration in the beaker was measured at the
151 beginning and ten seconds after the collection of the last time-series sample. The decay
152 in free chlorine concentration was less than 12% throughout each run. The chlorine
153 exposure (CT value; concentration of free chlorine multiplied by contact time) for each
154 sample, was given by integration of the time-dependent disinfectant concentration over
155 exposure time, assuming the first-order decay in free chlorine concentration between the
156 two time points.

157

158 *UV*

159 UV irradiation was performed in a collimated beam low-pressure UV system. The
160 UV system comprised an 18 W low-pressure UVC lamp (model TUV T8; Philips,
161 Netherlands), which emitted 253.7 nm light as a quasi-collimated beam³⁸. The fluence
162 rate was determined to be 116–136 $\mu\text{W cm}^{-2}$ by chemical actinometry³⁹. A 5 mL aliquot
163 of 1 mM PB spiked with 30 μL of virus stock was irradiated in a 20 mL beaker with
164 gentle stirring. A 400 μL aliquot was collected every 30 seconds. The collected samples
165 were stored at 4 °C until virus enumeration as specified above. The UV exposure (mJ
166 cm^{-2}) for each sample was determined as a product of the fluence rate and the
167 corresponding exposure time.

168

169 *Heat Treatment*

170 Heat treatment was conducted in a thermal cycler (GeneAmp PCR system 9700,
171 Applied Biosystems, USA). Five microliters of purified virus stock was spiked into
172 thin-wall PCR tubes containing 45 μL of 1 mM PB. The tubes were incubated at 50 °C
173 for either 20s, 40s, or 60s. The incubated tubes were immediately cooled down by
174 placing them on crushed ice, and samples were stored at 4 °C as specified above until
175 enumeration.

176 Estimation of Inactivation Rate Constants

177 Inactivation rate constants ($k_{\text{infectivity}}$) were estimated by fitting a pseudo-first-order

178 model for free chlorine and UV or a first-order model for heat (see Table S2) to the
179 corresponding experimental data, excluding those under the LoD. The rate constants
180 were determined based on the pooled data from all replicates as the slope of $\ln(N/N_0)$
181 versus disinfectant exposure (free chlorine and UV) or time (heat) by linear
182 least-squares regression, where N is the infectious virus concentration at time T (MPN
183 mL^{-1}), N_0 is the infectious virus concentration at time 0 (MPN mL^{-1}), both of which
184 were determined on the corresponding host cells.

185 Host attachment of E11 Treated by Free Chlorine

186 The capacity of E11 to bind to host cells was quantified, with a slight modification of
187 our previous report³³. Untreated and disinfected virus samples were diluted 10-fold in
188 maintenance medium. 500 μL of diluted virus samples were added to cell monolayers
189 (BGMK, RD, or A549) in 12-well plates for 1 h at 4°C. The cell monolayers were then
190 washed three times with 300 μL of phosphate-buffered saline (PBS, pH 7.4) per well to
191 remove unbound viruses and free RNA. 140 μL of PB was added to each well and
192 samples were stored at -20°C for a maximum of 24 h prior to RNA extraction. After
193 thawing, 560 μL of AVL buffer with carrier RNA, both taken from the QIAamp Viral
194 RNA Mini Kit (QIAGEN, Germany), were added to each well and incubated for 10 min
195 at room temperature, to lyse the bound viruses. The lysate was processed according to
196 the manufacturer's instruction to obtain RNA extracts in 40 μL of ultrapure water. The
197 RNA concentration was measured by reverse transcription digital PCR (RT-dPCR)
198 using reported primers and probe^{40,41} on QIAcuity dPCR 2-plex platform (QIAGEN) as
199 detailed in the SI.

200 The observed rate constants of attachment loss ($k_{\text{obs_attachment}}$) were determined based
201 on the pooled data from triplicate experiments as the slope of $\ln(GC/GC_0)$ versus CT
202 value by linear least-squares regression, where GC_0 and GC are the number of bound
203 viruses (measured as genome copies) before and after chlorine exposure, respectively.
204 Note that the difference in observed genome copy numbers between untreated and
205 disinfected samples stems from a reduction in bound viruses, as well as from the decay
206 of the targeted PCR segment due to exposure to free chlorine³³. To determine the net
207 rate constants for attachment loss ($k_{\text{attachment}}$), $k_{\text{obs_attachment}}$ was thus corrected by the

208 observed decay of the PCR-target ($k_{\text{PCR-target}}$), which was measured in sample aliquots
209 not included in the binding assay (see Eq.(1)).

$$k_{\text{attachment}} = k_{\text{obs_attachment}} - k_{\text{PCR-target}} \quad \#(1)$$

210

211 Flow Cytometric Analysis of Cell Receptors

212 Cells were washed with PBS, detached by 0.05% trypsin-EDTA (Gibco), and pelleted
213 in a 96-well U-bottom plate (Thermofisher Scientific, USA) at 10^5 cells per well by
214 centrifugation at $400 \times g$ for 2 min. Cells were washed twice in PBS and then stained
215 with $1 \mu\text{g/mL}$ of DAPI (Sigma-Aldrich) for 15 min at room temperature in the dark.
216 After being washed twice by staining buffer (PBS with 1% of bovine serum albumin),
217 cells were incubated with Fc receptor blocking solution (BD Pharmingen, USA) for 15
218 min at room temperature in the dark. Subsequently, cells were stained with
219 FITC-conjugated anti-human CD55 antibody (Biolegend, USA) ($2 \mu\text{g/mL}$) and
220 APC-conjugated anti-human $\beta 2$ -microglobulin ($\beta 2\text{M}$) antibody (Biolegend) (0.25
221 $\mu\text{g/mL}$), or isotype controls (FITC-conjugated mouse IgG1 (Biolegend) and APC mouse
222 IgG1-conjugated (Biolegend) for 20 min at 4°C in the dark. Stained cells were washed
223 twice with PBS and resuspended with $200 \mu\text{L}$ of PBS prior to immediate acquisition.
224 Data acquisition for all samples was performed on a Gallios flow cytometer (Beckman
225 Coulter) at the EPFL Flow Cytometry Core Facility, with a minimum of 10,000 cells
226 acquired per sample. Acquired data were analyzed in FloJo software version 10.8.0. Cell
227 doublets were excluded by single cell gating, and single cells were then gated based on
228 viability (DAPI) prior to analysis of cell receptor expression ($\text{CD55}^+ / \beta 2\text{M}^+$).
229 Unstained cells and those stained with isotype control antibodies were used to set
230 negative gates for fluorescence for each cell type.

231 Statistical Analyses

232 All statistical analyses were implemented in R-4.1.2⁴². Linear least-squares
233 regression was performed with the `{lm}` function to estimate inactivation rate constants
234 from the disinfection experiments. Inactivation rate constants of the different host cells

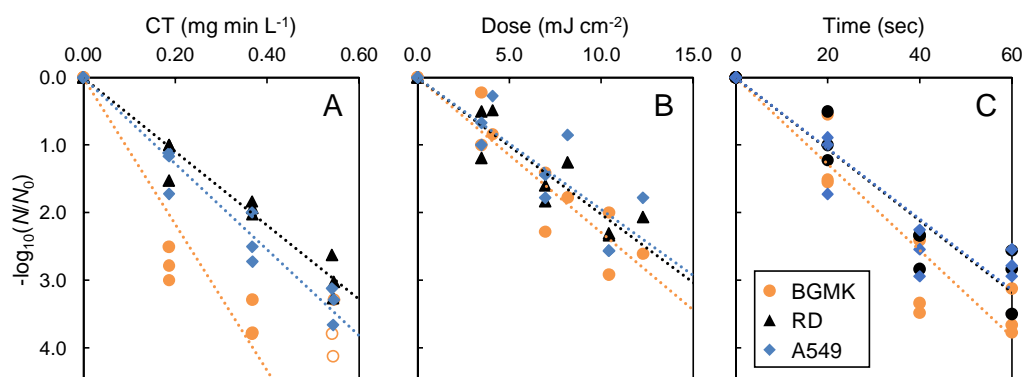
235 were compared by analysis of covariance (Type III) using {Anova} function in the car
236 package⁴³. If a significant effect of host cells was observed, a post-hoc analysis was
237 performed using {emtrends} function in the emmeans package⁴⁴ to determine which
238 pairs of host cells are significantly different. The alpha-type error was set at 0.05.

239 **Results and Discussion**

240 **Observed Kinetics of E11 Inactivation Enumerated by Different Host Cells**

241 Prior to conducting inactivation experiments, we ensured that all three host cells were
242 permissive to E11 infection. We found that each cell type produced high E11 titers,
243 (ranging from 6.9 – 7.9 log₁₀ MPN/mL; Table S1), suggesting that all the cells were
244 readily infected by E11.

245 To assess the impact of host cells on the observed kinetics of E11 inactivation,
246 untreated and disinfected samples were enumerated individually on the three different
247 host cells included in this work. The resulting inactivation curves are shown in Figure 1.
248 The observed inactivation efficiencies for free chlorine were higher for E11 samples
249 enumerated with BGMK cells compared with RD and A549 cells. For example, at a CT
250 0.18 mg min L⁻¹, E11 Gregory was inactivated by 2.8 log₁₀ on BGMK cells, compared
251 with the lower 1.2 and 1.3 log₁₀ seen on RD and A549 cells, respectively. (Figure 1A).
252 The observed inactivation rate constants ($k_{\text{infectivity}}$) were 25.0, 12.6, and 14.6 mg⁻¹ min⁻¹
253 L for BGMK, RD, A549 cells, respectively (Table 1). The inactivation rate constants for
254 BGMK cells were 2.0- and 1.7-fold higher than those for RD and A549 cells,
255 respectively, and these differences were statistically significant (p-value: 9.5×10^{-5}
256 (BGMK - RD) and 1.0×10^{-3} (BGMK - A549)). On the other hand, the choice of host
257 cell only led to small and not statistically significant differences in inactivation kinetics
258 of E11 treated by UV or heat (Figure 1B, C). These results demonstrate that the
259 observed inactivation kinetics of E11 depend on the host cells used for enumeration,
260 though the magnitude of the host cell effect depends on the disinfectant.



261

262 Figure 1 Inactivation of E11 by free chlorine (A), UV (B), and heat (C) measured on
 263 BGMK (orange circles), RD (black triangles), and A549 (blue diamonds) cells. Dashed
 264 lines show each regression line. Empty symbols indicate right-censored data and are
 265 plotted at the value of $-\log_{10}(LoD/N_0)$.

266

267 Table 1 Rate constants for the inactivation ($k_{infectivity}$) and loss of attachment ($k_{attachment}$)
 268 after treatment of E11 by free chlorine

Host cells	$k_{infectivity}$ ($\text{mg}^{-1} \text{min}^{-1} \text{L}$)	$k_{attachment}$ ($\text{mg}^{-1} \text{min}^{-1} \text{L}$)
BGMK	25.0	14.1
RD	12.6	9.0
A549	14.6	8.9

269

270

271

272 Potential Mechanism of Host Cell-Dependent Kinetics of Inactivation by Free 273 Chlorine

274 Free chlorine was previously shown to inhibit the ability of E11 to attach to BGМК
275 cells³³. We therefore investigated if the host cell-dependence of E11 inactivation
276 kinetics could be explained by a differential effect of free chlorine on host attachment to
277 the three cell types studied. Figure S1 shows the observed loss of attachment as a
278 function of CT values, and Table 1 shows the rate constants for loss of attachment
279 ($k_{\text{attachment}}$). The $k_{\text{attachment}}$ was 14.1, 9.0, and 8.9 mg⁻¹ min⁻¹ L for BGМК, RD, and A549
280 cells. This demonstrates that binding capability to BGМК cells was affected most
281 strongly.

282 This finding can be rationalized by considering the receptor profiles of the three host
283 cells. A flow cytometry analysis was used to characterize the presence of CD55, an
284 attachment receptor, and β 2M, a key subunit of the uncoating receptor FcRn, on each of
285 the host cells. Expression of these receptors on BGМК, RD, and A549 cells is shown in
286 Figure S2 and summarized in Table 2. The attachment receptor CD55 was expressed on
287 RD and A549 cells but was not detected on BGМК cells. This confirms a previous
288 finding, which reported that BGМК cells were negative for CD55 while RD cells were
289 positive²⁷. Similarly, β 2M was detected on RD and A549 cells, but not on BGМК cells.
290 Expression of β 2M on RD cells is consistent with a previous finding³⁰. These results
291 suggest that both RD and A549 cells can interact with E11 via CD55 and β 2M while
292 BGМК cells cannot. Given that BGМК cells replicated the untreated E11 as efficiently
293 as the other two host cells (Table S1), BGМК cells must possess alternative attachment
294 and uncoating receptors for E11. This further implies that E11 uses different motifs on
295 the viral capsid to interact with host cell receptors on BGМК cells than on RD or A549
296 cells. A preference of free chlorine for certain proteins of viral capsids has previously
297 been reported for phages^{31,45,46}. The greater effect of free chlorine on host attachment to
298 BGМК cells may thus stem from preferential oxidation of the binding motif for BGМК
299 compared to CD55.

300

301

Table 2 Expression of receptors on each of the host cells

Host cells	CD55	β 2M
BGMK	Negative	Negative
RD	Positive	Positive
A549	Positive	Positive

302

303 The difference in $k_{\text{attachment}}$ between BGMK and the other two host cells alone,
304 however, cannot explain the much larger difference in the $k_{\text{infectivity}}$ (Table 1). We
305 hypothesize that the rate of uncoating is also more affected in viruses enumerated on
306 BGMK cells compared to the other two cell types. Given the absence of β 2M on
307 BGMK cells (Table 2), E11 must use a different receptor and hence a different host
308 interaction site to successfully uncoat in BGMK cells. If this host interaction site is
309 more susceptible to degradation by chlorine, then this would lead to a faster loss of the
310 uncoating function between viruses enumerated on different host cells. This hypothesis
311 could not be tested in this study, because we were not able to quantitatively measure
312 virus internalization. A published assay²⁶ was tested but was not able to separate
313 between truly internalized and merely bound viruses (data not shown) in our
314 experimental conditions.

315 We do not expect the replicative function to be differentially affected in different host
316 cells. Loss of the replicative function can be regarded as the loss of intact RNA that can
317 be replicated and transcribed by cellular protein synthesis machinery. Given that the
318 repair of ssRNA within the host cells is unlikely, the intactness of RNA is dependent on
319 virus and treatment and independent of host cells. In fact, for UV, which dominantly
320 damages E11 replicative function^{33,47}, a similar $k_{\text{inactivation}}$ was observed regardless of
321 host cells, suggesting that a loss of replicative function affects all host cells equally.

322 Similar to free chlorine, heat was reported to strongly affect $k_{\text{attachment}}$ of E11³³.
323 Interestingly, the choice of host cell did not influence virus inactivation kinetics by heat.
324 A potential hypothesis is a difference in the damaging mechanism between free chlorine
325 and heat treatment. Previous studies found that mild heat treatment either causes the
326 capsid to dissociate into pentameric subassemblies⁴⁸ or induces conformational
327 rearrangement⁴⁹, both of which release enteroviral RNA to the outside of the capsid^{48,49}.

328 Disassembled or rearranged capsids would not be expected to interact with any host cell
329 receptors, such that the attachment of E11 to all host cells, and hence the infectivity of
330 E11, would decline at an equal rate.

331

332

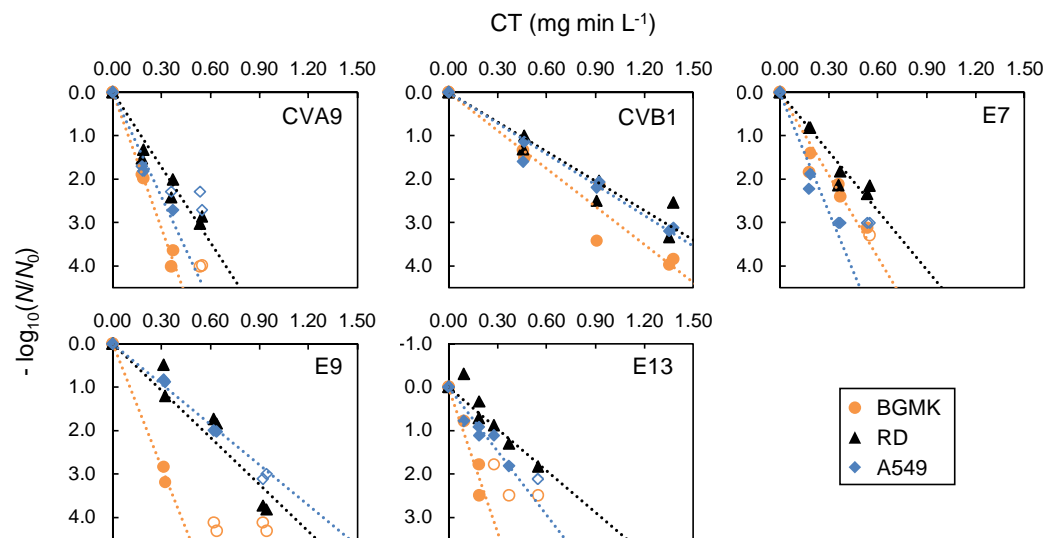
333

334 Effect of Host Cells on the Inactivation Kinetics of Other Serotypes of the
335 *Enterovirus* Genus

336 A panel of enteroviruses (CVA9, CVB1, E7, E9, and E13), which were reported to be
337 prevalent in European sewage⁵⁰, was tested for their ability to infect the three host cells
338 (Table S1). The results suggested that these viruses can propagate in BGMK cells as
339 well as RD and A549 cells, despite the lack of CD55 and β 2M. Subsequently, the five
340 viruses were examined for host cell-dependence in their inactivation kinetics by free
341 chlorine. Inactivation curves were determined for each combination of the virus and the
342 host cells (Figure 2). The effect of host cells on observed inactivation rate constants was
343 significant for all the tested viruses, except for CVB1. The effect size ranged from a 1.3-
344 to a 3.5-fold change in $k_{\text{infectivity}}$, depending on the serotype. The observed inactivation
345 on BGMK cells was significantly faster than that on RD and A549 cells for CVA9
346 (p-value: 4.8×10^{-5} (BGMK-RD) and 3.8×10^{-2} (BGMK-A549)), E9 (p-value: $3.4 \times$
347 10^{-4} (BGMK-RD) and 3.8×10^{-2} (BGMK-A549)), and E13 (p-value: 2.2×10^{-4}
348 (BGMK-RD) and 1.1×10^{-3} (BGMK-A549)). A significant difference between RD and
349 A549 cells was only observed for E7 (p-value: 6.9×10^{-3}).

350 We attempted to rationalize these observations by considering the receptor profiles of
351 the three host cells (Table S3) and the receptor usage of each serotype (Table S4). CVA9
352 and E9 were reported to use α V β 3 as an attachment receptor, which is expressed on all
353 cell types used. This attachment receptor can thus not be implicated as the cause for host
354 cell-dependent inactivation kinetics. These viruses furthermore use FcRn for uncoating,
355 which is absent from BGMK cells. As discussed above for E11, CVA9 and E9 must thus
356 rely on an alternative uncoating receptor on BGMK cells, which may lead to the
357 observed increase in sensitivity to free chlorine. E13 was reported to use CD55 as an
358 attachment receptor and FcRn as an uncoating receptor, and thus has the same receptor
359 usage as E11. It is then not surprising that this virus exhibited a similar host
360 cell-dependence in its inactivation kinetics as E11. Interestingly, however, the same
361 receptors are also used by E7, which did not exhibit significantly faster inactivation
362 kinetics when using BGMK cells as the host. This may be rationalized by reports that
363 E7 can also enter cells by clathrin-mediated endocytosis⁵¹. The significant difference
364 between inactivation rates measured on RD and A549 cells for E7, however, remains to

365 be investigated. Finally, further investigation is also required to understand the
366 comparable inactivation rates of CVB1 on all host cells. A possible explanation is this
367 virus' use of the coxsackievirus and adenovirus receptor (CAR), which works
368 bi-functionally as an attachment and uncoating receptor for Group B coxsackieviruses⁵².
369 CAR was reported to be expressed on all three host cells used herein, though the
370 expression level is reported differently among studies^{27,53}. The similarity of the major
371 infection route may explain the similar rate constants among the host cells tested here.
372 In summary, the host cell-dependent inactivation kinetics for free chlorine was
373 observed for several serotypes of the *Enterovirus* genus. Further research is needed to
374 conclusively determine if the magnitude of the difference is associated with receptor
375 usage of the tested viruses and the availability of attachment and uncoating receptors
376 expressed by each of the host cells.



377
378 Figure 2 Inactivation of a panel of enteroviruses by free chlorine determined by
379 enumeration on BGMK (orange circles), RD (black triangles), and A549 (blue
380 diamonds) cells. Dashed lines show each regression line. Empty symbols indicate
381 right-censored data and are plotted at the value of $-\log_{10}(LoD/N_0)$.
382

383 Environmental Implications

384 This work revealed host cell-dependent kinetics of enterovirus after inactivation by
385 free chlorine and suggested potential mechanistic contributions of host cell receptor
386 profiles to this phenomenon. Furthermore, data indicate that host cell-dependent
387 inactivation kinetics are observed for a range of serotypes of the *Enterovirus* genus.

388 To date, the classic method for assessing the virucidal efficacy of disinfectants is to
389 select any single cell type permissible to infection by the tested virus. Our results
390 caution against this approach, and instead encourage the use of multiple cell types with
391 different receptor profiles. This would reduce the risk of inactivation efficiencies being
392 over- or underestimated, especially for disinfectants damaging the capsid in a selective
393 manner (e.g., chlorine dioxide³¹). Moreover, an appropriate rationale is necessary to
394 select the host cells used to evaluate disinfection efficiency. For example, this study
395 shows that RD cells can provide more conservative estimates of inactivation efficiency
396 (Figure 2) and observed infectious concentration for echoviruses than BGMK cells
397 (Table S1). A possible approach more representative of human infection may be the use
398 of host cells closer to the gastrointestinal tract (e.g., Caco-2 and HT29 cells), or
399 enteroids⁵⁴ as an *ex vivo* model of the human intestinal epithelium. Also, *in vivo*
400 disinfection experiments (e.g. those performed by Zhang et al.⁵⁵) compared with *in*
401 *vitro* experiments could aid in understanding the meaning of observed inactivation
402 efficiency. Collectively, these new approaches will improve our interpretation of the
403 observed inactivation *in vitro* and understand “true” inactivation kinetics by
404 disinfection.

405

406 **Acknowledgment**

407 This work was funded in part by the JSPS Overseas Challenge Program for Young
408 Researchers, the Young Researchers Exchange Programme between Japan and
409 Switzerland (EGJP_04-042020), a JSPS Overseas Research Fellowships to S.T., and by
410 EPFL discretionary funds. We thank the EPFL Flow Cytometry Core Facility for access
411 to instruments and technical help. We also thank Soile Blomqvist and Carita
412 Savolainen-Kopra (Finnish National Institute for Health and Welfare) for providing
413 environmental enterovirus isolates.

414 **Supporting Information**

415 The Supporting Information is available at XXXXXX.

- 416 • RT-dPCR methods used; Infectious virus concentration of virus stocks
417 enumerated on each of host cells; Inactivation models; Expression of receptors
418 for each of host cells; reported receptors for enteroviruses; CD55 and β 2M
419 expression on BGMK, RD, and A549 cells; Decay of virus functions with free
420 chlorine.

421 **Data availability**

422 All data discussed in this manuscript will be made available on zenodo upon
423 acceptance of the manuscript.

424

425 References

- 426 (1) Bubba, L.; Broberg, E. K.; Jasir, A.; Simmonds, P.; Harvala, H.;
427 Redlberger-Fritz, M.; Nikolaeva-Glomb, L.; Havlíčková, M.; Rainetova, P.;
428 Fischer, T. K.; Midgley, S. E.; Epštein, J.; Blomqvist, S.; Böttcher, S.; Keeren, K.;
429 Bujaki, E.; Farkas, Á.; Baldvinsdóttir, G. E.; Morley, U.; De Gascun, C.;
430 Pellegrinelli, L.; Piralla, A.; Martinuka, O.; Zamjatina, N.; Griškevičius, A.;
431 Nguyen, T.; Dudman, S. G.; Numanovic, S.; Wiczorek, M.; Guiomar, R.; Costa,
432 I.; Cristina, T.; Bopegamage, S.; Pastuchova, K.; Berginc, N.; Cabrerizo, M.;
433 González-Sanz, R.; Zakikhany, K.; Hauzenberger, E.; Benschop, K.; Duizer, E.;
434 Dunning, J.; Celma, C.; McKenna, J.; Feeney, S.; Templeton, K.; Moore, C.;
435 Cottrell, S. Circulation of Non-Polio Enteroviruses in 24 EU and EEA Countries
436 between 2015 and 2017: A Retrospective Surveillance Study. *Lancet Infect. Dis.*
437 **2020**, *20* (3), 350–361. [https://doi.org/10.1016/S1473-3099\(19\)30566-3](https://doi.org/10.1016/S1473-3099(19)30566-3).
- 438 (2) Haramoto, E.; Kitajima, M.; Hata, A.; Torrey, J. R.; Masago, Y.; Sano,
439 D.; Katayama, H. A Review on Recent Progress in the Detection Methods and
440 Prevalence of Human Enteric Viruses in Water. *Water Res.* **2018**, *135*, 168–186.
441 <https://doi.org/10.1016/j.watres.2018.02.004>.
- 442 (3) Lee, S. H.; Kim, S. J. Detection of Infectious Enteroviruses and
443 Adenoviruses in Tap Water in Urban Areas in Korea. *Water Res.* **2002**, *36* (1),
444 248–256. [https://doi.org/10.1016/S0043-1354\(01\)00199-3](https://doi.org/10.1016/S0043-1354(01)00199-3).
- 445 (4) Cromeans, T. L.; Kahler, A. M.; Hill, V. R. Inactivation of
446 Adenoviruses, Enteroviruses, and Murine Norovirus in Water by Free Chlorine and
447 Monochloramine. *Appl. Environ. Microbiol.* **2010**, *76* (4), 1028–1033.
448 <https://doi.org/10.1128/AEM.01342-09>.
- 449 (5) Floyd, R.; Sharp, D. G.; Johnson, J. D. Inactivation by Chlorine of
450 Single Poliovirus Particles in Water. *Environ. Sci. Technol.* **1979**, *13* (4), 438–442.
451 <https://doi.org/10.1021/es60152a005>.
- 452 (6) Payment, P.; Tremblay, M.; Trudel, M. Relative Resistance to Chlorine
453 of Poliovirus and Coxsackievirus Isolates from Environmental Sources and
454 Drinking Water. *Appl. Environ. Microbiol.* **1985**, *49* (4), 981–983.
455 <https://doi.org/10.1128/aem.49.4.981-983.1985>.
- 456 (7) Sobsey, M. D.; Fuji, T.; Shields, P. A. Inactivation of Hepatitis A Virus
457 and Model Viruses in Water by Free Chlorine and Monochloramine. *Water Sci.*
458 *Technol.* **1988**, *20* (11–12), 385–391. <https://doi.org/10.2166/wst.1988.0310>.
- 459 (8) Torii, S.; Corre, M.-H.; Miura, F.; Itamochi, M.; Haga, K.; Katayama,

- 460 K.; Katayama, H.; Kohn, T. Genotype-Dependent Kinetics of Enterovirus
461 Inactivation by Free Chlorine and Ultraviolet (UV) Irradiation. *Water Res.* **2022**,
462 *220*, 118712. <https://doi.org/10.1016/j.watres.2022.118712>.
- 463 (9) Weidenkopf, S. J. Inactivation of Type 1 Poliomyelitis Virus with
464 Chlorine. *Virology* **1958**, *5* (1), 56–67.
465 [https://doi.org/10.1016/0042-6822\(58\)90005-9](https://doi.org/10.1016/0042-6822(58)90005-9).
- 466 (10) Rachmadi, A. T.; Kitajima, M.; Kato, T.; Kato, H.; Okabe, S.; Sano, D.
467 Required Chlorination Doses to Fulfill the Credit Value for Disinfection of Enteric
468 Viruses in Water: A Critical Review. *Environ. Sci. Technol.* **2020**, *54* (4),
469 2068–2077. <https://doi.org/10.1021/acs.est.9b01685>.
- 470 (11) Barron, A. L.; Olshevsky, C.; Cohen, M. M. Characteristics of the
471 BGM Line of Cells from African Green Monkey Kidney. *Arch. Für Gesamte*
472 *Virusforsch.* **1970**, *32* (4), 389–392. <https://doi.org/10.1007/BF01250067>.
- 473 (12) Black, S.; Thurston, J. A.; Gerba, C. P. Determination of Ct Values for
474 Chlorine of Resistant Enteroviruses. *J. Environ. Sci. Health - Part Toxic/Hazardous*
475 *Subst. Environ. Eng.* **2009**, *44* (4), 336–339.
476 <https://doi.org/10.1080/10934520802659653>.
- 477 (13) Gerba, C. P.; Gramos, D. M.; Nwachuku, N. Comparative Inactivation
478 of Enteroviruses and Adenovirus 2 by UV Light. *Appl. Environ. Microbiol.* **2002**,
479 *68* (10), 5167–5169. <https://doi.org/10.1128/AEM.68.10.5167-5169.2002>.
- 480 (14) Kahler, A. M.; Cromeans, T. L.; Roberts, J. M.; Hill, V. R. Effects of
481 Source Water Quality on Chlorine Inactivation of Adenovirus, Coxsackievirus,
482 Echovirus, and Murine Norovirus. *Appl. Environ. Microbiol.* **2010**, *76* (15),
483 5159–5164. <https://doi.org/10.1128/AEM.00869-10>.
- 484 (15) Meister, S.; Verbyla, M. E.; Klinger, M.; Kohn, T. Variability in
485 Disinfection Resistance between Currently Circulating Enterovirus B Serotypes
486 and Strains. *Environ. Sci. Technol.* **2018**, *52* (6), 3696–3705.
487 <https://doi.org/10.1021/acs.est.8b00851>.
- 488 (16) Shirasaki, N.; Matsushita, T.; Matsui, Y.; Koriki, S. Suitability of
489 Pepper Mild Mottle Virus as a Human Enteric Virus Surrogate for Assessing the
490 Efficacy of Thermal or Free-Chlorine Disinfection Processes by Using Infectivity
491 Assays and Enhanced Viability PCR. *Water Res.* **2020**, *186*.
492 <https://doi.org/10.1016/j.watres.2020.116409>.
- 493 (17) Torii, S.; Miura, F.; Itamochi, M.; Haga, K.; Katayama, K.; Katayama,
494 H. Impact of the Heterogeneity in Free Chlorine, UV254, and Ozone
495 Susceptibilities among Coxsackievirus B5 on the Prediction of the Overall

- 496 Inactivation Efficiency. *Environ. Sci. Technol.* **2021**, *55* (5), 3156–3164.
497 <https://doi.org/10.1021/acs.est.0c07796>.
- 498 (18) Dahling, D. R.; Wright, B. A. Optimization of the BGM Cell Line
499 Culture and Viral Assay Procedures for Monitoring Viruses in the Environment.
500 *Appl. Environ. Microbiol.* **1986**, *51* (4), 790–812.
501 <https://doi.org/10.1128/aem.51.4.790-812.1986>.
- 502 (19) Fout, G. S.; Cashdollar, J. L.; Griffin, S. M.; Brinkman, N. E.;
503 Varughese, E. A.; Parshionikar, S. U. EPA Method 1615. Measurement of
504 Enterovirus and Norovirus Occurrence in Water by Culture and RT-QPCR. Part III.
505 Virus Detection by RT-QPCR. *J. Vis. Exp.* **2016**, No. 107, e52646.
506 <https://doi.org/10.3791/52646>.
- 507 (20) Pecson, B. M.; Darby, E.; Danielson, R.; Dearborn, Y.; Giovanni, G.
508 D.; Jakubowski, W.; Leddy, M.; Lukasik, G.; Mull, B.; Nelson, K. L.; Olivieri, A.;
509 Rock, C.; Slifko, T. Distributions of Waterborne Pathogens in Raw Wastewater
510 Based on a 14-Month, Multi-Site Monitoring Campaign. *Water Res.* **2022**, *213*,
511 118170. <https://doi.org/10.1016/j.watres.2022.118170>.
- 512 (21) Rezaikin, A. V.; Novoselov, A. V.; Sergeev, A. G.; Fadeyev, F. A.;
513 Lebedev, S. V. Two Clusters of Mutations Map Distinct Receptor-Binding Sites of
514 Echovirus 11 for the Decay-Accelerating Factor (CD55) and for Canyon-Binding
515 Receptors. *Virus Res.* **2009**, *145* (1), 74–79.
516 <https://doi.org/10.1016/j.virusres.2009.06.004>.
- 517 (22) Smith; Craft, DW; Shiromoto, RS; Yan, PO. Alternative Cell Line for
518 Virus Isolation. *J. Clin. Microbiol.* **1986**, *24* (2), 265–268.
519 <https://doi.org/10.1128/jcm.24.2.265-268.1986>.
- 520 (23) Zhong, Q.; Carratalà, A.; Shim, H.; Bachmann, V.; Jensen, J. D.; Kohn,
521 T. Resistance of Echovirus 11 to ClO₂ Is Associated with Enhanced Host Receptor
522 Use, Altered Entry Routes, and High Fitness. *Environ. Sci. Technol.* **2017**, *51* (18),
523 10746–10755. <https://doi.org/10.1021/acs.est.7b03288>.
- 524 (24) Bergelson, J. M.; Chan, M.; Solomon, K. R.; John, N. F. S. T.; Lin, H.;
525 Finberg, R. W. Decay-Accelerating Factor (CD55), a
526 Glycosylphosphatidylinositol-Anchored Complement Regulatory Protein, Is a
527 Receptor for Several Echoviruses. *Proc. Natl. Acad. Sci.* **1994**, *91* (June),
528 6245–6248.
- 529 (25) Novoselov, A. V.; Rezaikin, A. V.; Sergeev, A. G.; Fadeyev, F. A.;
530 Grigoryeva, J. V.; Sokolova, Z. I. A Single Amino Acid Substitution Controls
531 DAF-Dependent Phenotype of Echovirus 11 in Rhabdomyosarcoma Cells. *Virus*

- 532 *Res.* **2012**, *166* (1), 87–96. <https://doi.org/10.1016/j.virusres.2012.03.007>.
- 533 (26) Zhao, X.; Zhang, G.; Liu, S.; Chen, X.; Peng, R.; Dai, L.; Qu, X.; Li,
534 S.; Song, H.; Gao, Z.; Yuan, P.; Liu, Z.; Li, C.; Shang, Z.; Li, Y.; Zhang, M.; Qi, J.;
535 Wang, H.; Du, N.; Wu, Y.; Bi, Y.; Gao, S.; Shi, Y.; Yan, J.; Zhang, Y.; Xie, Z.; Wei,
536 W.; Gao, G. F. Human Neonatal Fc Receptor Is the Cellular Uncoating Receptor
537 for Enterovirus B. *Cell* **2019**, *177* (6), 1553-1565.e16.
538 <https://doi.org/10.1016/j.cell.2019.04.035>.
- 539 (27) Hsu, K. H.; Lonberg-Holm, K.; Alstein, B.; Crowell, R. L. A
540 Monoclonal Antibody Specific for the Cellular Receptor for the Group B
541 Coxsackieviruses. *J. Virol.* **1988**, *62* (5), 1647–1652.
542 <https://doi.org/10.1128/jvi.62.5.1647-1652.1988>.
- 543 (28) Morosky, S.; Wells, A. I.; Lemon, K.; Evans, A. S.; Schamus, S.;
544 Bakkenist, C. J.; Coyne, C. B. The Neonatal Fc Receptor Is a Pan-Echovirus
545 Receptor. *Proc. Natl. Acad. Sci.* **2019**, *116* (9), 3758–3763.
546 <https://doi.org/10.1073/pnas.1817341116>.
- 547 (29) Chevaliez, S.; Balanant, J.; Maillard, P.; Lone, Y.-C.; Lemonnier, F. A.;
548 Delpeyroux, F. Role of Class I Human Leukocyte Antigen Molecules in Early
549 Steps of Echovirus Infection of Rhabdomyosarcoma Cells. *Virology* **2008**, *381* (2),
550 203–214.
- 551 (30) Ward, T.; Powell, R. M.; Pipkin, P. A.; Evans, D. J.; Minor, P. D.;
552 Almond, J. W. Role for B2-Microglobulin in Echovirus Infection of
553 Rhabdomyosarcoma Cells. *J. Virol.* **1998**, *72* (7), 5360–5365.
- 554 (31) Wigginton, K. R.; Pecson, B. M.; Sigstam, T.; Bosshard, F.; Kohn, T.
555 Virus Inactivation Mechanisms: Impact of Disinfectants on Virus Function and
556 Structural Integrity. *Environ. Sci. Technol.* **2012**, *46* (21), 12069–12078.
557 <https://doi.org/10.1021/es3029473>.
- 558 (32) Torrey, J.; von Gunten, U.; Kohn, T. Differences in Viral Disinfection
559 Mechanisms as Revealed by Quantitative Transfection of Echovirus 11 Genomes.
560 *Appl. Environ. Microbiol.* **2019**, *85* (14), 1–14.
561 <https://doi.org/10.1128/AEM.00961-19>.
- 562 (33) Zhong, Q.; Carratalà, A.; Ossola, R.; Bachmann, V.; Kohn, T.
563 Cross-Resistance of UV- or Chlorine Dioxide-Resistant Echovirus 11 to Other
564 Disinfectants. *Front. Microbiol.* **2017**, *8* (OCT), 1–12.
565 <https://doi.org/10.3389/fmicb.2017.01928>.
- 566 (34) Guo, H.; Chu, X.; Hu, J. Effect of Host Cells on Low- and
567 Medium-Pressure UV Inactivation of Adenoviruses. *Appl. Environ. Microbiol.*

- 568 **2010**, 76 (21), 7068–7075. <https://doi.org/10.1128/AEM.00185-10>.
- 569 (35) Torii, S.; Itamochi, M.; Katayama, H. Inactivation Kinetics of
570 Waterborne Virus by Ozone Determined by a Continuous Quench Flow System.
571 *Water Res.* **2020**, 186, 116291. <https://doi.org/10.1016/j.watres.2020.116291>.
- 572 (36) Ferguson, M.; Ihrle, J. MPN: Most Probable Number and Other
573 Microbial Enumeration Techniques. **2019**.
- 574 (37) Clesceri, L. S.; Greenberg, A. E.; Trussell, R. R. *Standard Methods for*
575 *the Examination of Water and Wastewater*; 1989.
- 576 (38) Mattle, M. J.; Kohn, T. Inactivation and Tailing during UV254
577 Disinfection of Viruses: Contributions of Viral Aggregation, Light Shielding
578 within Viral Aggregates, and Recombination. *Environ. Sci. Technol.* **2012**, 46 (18),
579 10022–10030. <https://doi.org/10.1021/es302058v>.
- 580 (39) Rahn, R. O. Potassium Iodide as a Chemical Actinometer for 254 Nm
581 Radiation: Use of Lodate as an Electron Scavenger. *Photochem. Photobiol.* **1997**,
582 66 (4), 450–455. <https://doi.org/10.1111/j.1751-1097.1997.tb03172.x>.
- 583 (40) Monpoeho, S.; Dehee, A.; Mignotte, B.; Schwartzbrod, L.; Marechal,
584 V.; Nicolas, J.-C.; Billaudel, S.; Ferre, V. Quantification of Enterovirus RNA in
585 Sludge Samples Using Single Tube Real-Time RT-PCR. *Biotechniques* **2000**, 29
586 (1), 88–93.
- 587 (41) Tsai, Y.-L.; Sobsey, M. D.; Sangermano, L. R.; Palmer, C. J. Simple
588 Method of Concentrating Enteroviruses and Hepatitis A Virus from Sewage and
589 Ocean Water for Rapid Detection by Reverse Transcriptase-Polymerase Chain
590 Reaction. *Appl. Environ. Microbiol.* **1993**, 59 (10), 3488–3491.
- 591 (42) R Core Team. R: A Language and Environment for Statistical
592 Computing, 2021.
- 593 (43) Fox, J.; Weisberg, S.; Adler, D.; Bates, D.; Baud-Bovy, G.; Ellison, S.;
594 Firth, D.; Friendly, M.; Gorjanc, G.; Graves, S. Package ‘Car.’ *Vienna R Found.*
595 *Stat. Comput.* **2012**, 16.
- 596 (44) Lenth, R.; Singmann, H.; Love, J.; Buerkner, P.; Herve, M. Emmeans:
597 Estimated Marginal Means, Aka Least-Squares Means. *R Package Version* **2018**, 1
598 (1), 3.
- 599 (45) Choe, J. K.; Richards, D. H.; Wilson, C. J.; Mitch, W. A. Degradation
600 of Amino Acids and Structure in Model Proteins and Bacteriophage MS2 by
601 Chlorine, Bromine, and Ozone. *Environ. Sci. Technol.* **2015**, 49 (22), 13331–13339.
602 <https://doi.org/10.1021/acs.est.5b03813>.
- 603 (46) Ye, Y.; Chang, P. H.; Hartert, J.; Wigginton, K. R. Reactivity of

- 604 Enveloped Virus Genome, Proteins, and Lipids with Free Chlorine and UV254.
605 *Environ. Sci. Technol.* **2018**, 52 (14), 7698–7708.
606 <https://doi.org/10.1021/acs.est.8b00824>.
- 607 (47) Young, S.; Torrey, J.; Bachmann, V.; Kohn, T. Relationship Between
608 Inactivation and Genome Damage of Human Enteroviruses Upon Treatment by
609 UV254, Free Chlorine, and Ozone. *Food Environ. Virol.* **2020**, 12 (1), 20–27.
610 <https://doi.org/10.1007/s12560-019-09411-2>.
- 611 (48) Kotecha, A.; Seago, J.; Scott, K.; Burman, A.; Loureiro, S.; Ren, J.;
612 Porta, C.; Ginn, H. M.; Jackson, T.; Perez-Martin, E. Structure-Based Energetics of
613 Protein Interfaces Guides Foot-and-Mouth Disease Virus Vaccine Design. *Nat.*
614 *Struct. Mol. Biol.* **2015**, 22 (10), 788–794.
- 615 (49) Levy, H. C.; Bostina, M.; Filman, D. J.; Hogle, J. M. Catching a Virus
616 in the Act of RNA Release: A Novel Poliovirus Uncoating Intermediate
617 Characterized by Cryo-Electron Microscopy. *J. Virol.* **2010**, 84 (9), 4426–4441.
- 618 (50) Larivé, O.; Brandani, J.; Dubey, M.; Kohn, T. An Integrated Cell
619 Culture Reverse Transcriptase Quantitative PCR (ICC-RTqPCR) Method to
620 Simultaneously Quantify the Infectious Concentrations of Eight Environmentally
621 Relevant Enterovirus Serotypes. *J. Virol. Methods* **2021**, 296 (June).
622 <https://doi.org/10.1016/j.jviromet.2021.114225>.
- 623 (51) Kim, C.; Bergelson, J. M. Echovirus 7 Entry into Polarized Caco-2
624 Intestinal Epithelial Cells Involves Core Components of the Autophagy Machinery.
625 *J. Virol.* **2014**, 88 (1), 434–443.
- 626 (52) Bergelson, J. M.; Cunningham, J. A.; Droguett, G.; Kurt-Jones, E. A.;
627 Krithivas, A.; Hong, J. S.; Horwitz, M. S.; Crowell, R. L.; Finberg, R. W. Isolation
628 of a Common Receptor for Coxsackie B Viruses and Adenoviruses 2 and 5.
629 *Science* **1997**, 275 (5304), 1320–1323.
630 <https://doi.org/10.1126/science.275.5304.1320>.
- 631 (53) Carson, S. D.; Kim, K.-S.; Pirruccello, S. J.; Tracy, S.; Chapman, N. M.
632 Endogenous Low-Level Expression of the Coxsackievirus and Adenovirus
633 Receptor Enables Coxsackievirus B3 Infection of RD Cells. *Journal of General*
634 *Virology*, 2007, 88, 3031–3038.
- 635 (54) Drummond, C. G.; Bolock, A. M.; Ma, C.; Luke, C. J.; Good, M.;
636 Coyne, C. B. Enteroviruses Infect Human Enteroids and Induce Antiviral
637 Signaling in a Cell Lineage-Specific Manner. *Proceedings of the National*
638 *Academy of Sciences*, 2017, 114, 1672–1677.
- 639 (55) Zhang, M.; Ghosh, S.; Li, M.; Altan-Bonnet, N.; Shuai, D.

640 Vesicle-Cloaked Rotavirus Clusters Are Environmentally Persistent and Resistant
641 to Free Chlorine Disinfection. *Environ. Sci. Technol.* **2022**.
642 <https://doi.org/10.1021/acs.est.2c00732>.
643